iScience

CellPress
OPEN ACCESS

Article

Development of luciferase-based highly sensitive reporters that detect ER-associated protein biogenesis abnormalities

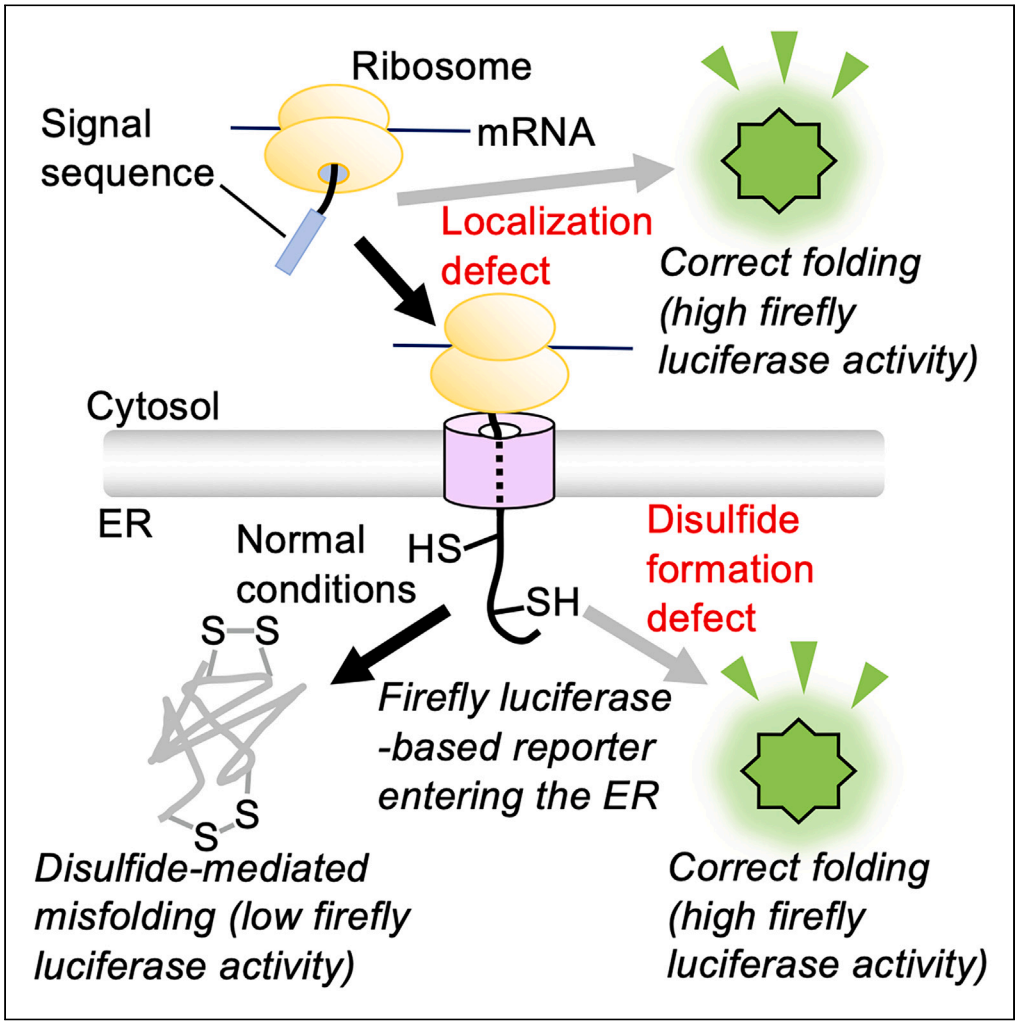

Hiroshi Kadokura, Nanshi Harada, Satoshi Yamaki, ..., Hideki Taguchi, Kenji Kohno, Kenji Inaba

kadokura.h.3c47@m.isct.ac.jp

Highlights

We engineered firefly luciferase to detect protein biogenesis abnormalities at the ER

The reporter proteins exhibited disulfide-mediated misfolding under normal conditions

The reporter system identified defects in disulfide bond formation or ER localization

It detected a localization defect induced by an inhibitor of virus receptor synthesis

Kadokura et al., iScience 27, 111189
November 15, 2024
https://doi.org/10.1016/j.isci.2024.111189

iScience

CellPress
OPEN ACCESS

Article

Development of luciferase-based highly sensitive reporters that detect ER-associated protein biogenesis abnormalities

Hiroshi Kadokura,[1,2,3,8,*] Nanshi Harada,[1] Satoshi Yamaki,[1] Naoya Hirai,[1,3] Ryusuke Tsukuda,[1] Kota Azuma,[1] Yuta Amagai,[1,6] Daisuke Nakamura,[2] Kota Yanagitani,[2,4] Hideki Taguchi,[3] Kenji Kohno,[2,5] and Kenji Inaba[1,6,7]

SUMMARY

Localization to the endoplasmic reticulum (ER) and subsequent disulfide bond formation are crucial processes governing the biogenesis of secretory pathway proteins in eukaryotes. Hence, comprehending the mechanisms underlying these processes is important. Here, we have engineered firefly luciferase (FLuc) as a tool to detect deficiencies in these processes within mammalian cells. To achieve this, we introduced multiple cysteine substitutions into FLuc and targeted it to the ER. The reporter exhibited FLuc activity in response to defects in protein localization or disulfide bond formation within the ER. Notably, this system exhibited outstanding sensitivity, reproducibility, and convenience in detecting abnormalities in these processes. We applied this system to observe a protein translocation defect induced by an inhibitor of HIV receptor biogenesis. Moreover, utilizing the system, we showed that modulating LMF1 levels dramatically impacted the ER's redox environment, confirming that LMF1 plays some critical role in the redox control of the ER.

INTRODUCTION

Protein translocation into the endoplasmic reticulum (ER) or the ER membrane is a decisive step in the biosynthesis of secretory pathway proteins.[1,2] Additionally, the folding and functionality of many of these proteins necessitate the formation of proper disulfide bonds. Accordingly, disruptions in these processes can result in pathological conditions.[3,4] Thus, understanding the mechanisms governing their ER localization and subsequent disulfide bond formation is highly important. Despite the extensive accumulation of information regarding these processes, their detailed mechanisms remain unclear.[1–3,5–8]

In *Escherichia coli*, a chromosomally encoded MalF-LacZ fusion expresses β-galactosidase activity when there is a deficiency in protein disulfide bond formation or protein localization to the cell envelope.[9] The utilization of this reporter and similar ones has contributed to our understanding of protein localization and folding in the bacterial cell envelope[10–14] and the discovery of compounds hindering the anaerobic growth of gram-negative bacteria through a new mode of action.[15] In MalF-LacZ, β-galactosidase (LacZ) is fused to a periplasmic loop of a membrane protein MalF, resulting in its localization to the periplasmic side of the cytoplasmic membrane. There, β-galactosidase's 16 cysteines (normally in a reduced state in the cytoplasm) undergo oxidation through the disulfide bond formation system of *E. coli*,[9,16] resulting in the improper folding and nearly complete inactivation of the enzyme. However, if there is a defect in protein disulfide bond formation or localization system, a portion of the β-galactosidase evades the action of disulfide bond-forming enzymes and adopts an enzymatically active conformation (Figure S1). MalF-LacZ, thereby, serves as a highly sensitive indicator of defects in these processes.[9,12,14]

Fluorescent protein derivatives equipped with a detector unit have proven effective in observing specific molecules or events in living mammalian cells. As these detection units are positioned on the surface of folded proteins, their readouts are generally reversible, rendering them valuable sensors of intracellular changes.[17,18] For example, roGFP has a pair of redox active cysteines on green fluorescence protein (GFP). The excitation properties of roGFP vary between the dithiol (reduced) and disulfide (oxidized) states, enabling real-time ratiometric imaging of redox fluctuations in the cytosol.[18–20]

To assess redox changes in the highly oxidative ER environment, a single amino acid was inserted adjacent to cysteine 147 in the roGFP β-barrel, resulting in roGFPiX, where X represents the inserted amino acid. This modification destabilized the Cys147-Cys204 disulfide in

[1]Institute of Multidisciplinary Research for Advanced Materials, Tohoku University, Sendai, Miyagi 980-8577, Japan
[2]Institute for Research Initiatives, Nara Institute of Science and Technology, Ikoma, Nara 630-0192, Japan
[3]Cell Biology Center, Institute of Integrated Research, Institute of Science Tokyo, Yokohama, Kanagawa 226-8501, Japan
[4]Graduate School of Frontier Biosciences, Osaka University, Suita, Osaka 565-0871, Japan
[5]Graduate School of Science, University of Hyogo, Harima Science Garden City, Hyogo 678-1297, Japan
[6]Medical Institute of Bioregulation, Kyushu University, Fukuoka, Fukuoka 812-8582, Japan
[7]Core Research for Evolutional Science and Technology (CREST), Japan Agency for Medical Research and Development (AMED), Chiyoda-ku, Tokyo 100-0004, Japan
[8]Lead contact
*Correspondence: kadokura.h.3c47@m.isct.ac.jp
https://doi.org/10.1016/j.isci.2024.111189

roGFPiX, yielding a less reducing protein suitable for detecting redox variations within the oxidizing ER environment.[21,22] However, the application of this roGFP mutant for detecting redox changes poses challenges due to its negative impact on fluorescent intensity, compromising sensitivity.[23] While increased excitation can mitigate the reduced fluorescence, it introduces issues such as photo-toxicity, disturbance of the redox environment, and strong autofluorescence, making it hard to obtain reliable data.[23] These problems were addressed by employing the lifetime measurement of roGFPiE, as the dithiol and disulfide states of the roGFP mutant exhibit significantly different fluorescence lifetimes. However, this method necessitates specialized equipment capable of measuring fluorescence decay within 10×10^{-9} s.[23] Furthermore, the stability and fluorescent intensity of ER-localized roGFPiL were enhanced by introducing mutations known to stabilize GFP.[24] Nevertheless, a great care is required during measurements due to considerable fluctuations in readouts under a given condition, often demanding repeated measurements to ensure data reliability.[25,26]

It is widely acknowledged that reporter assays utilizing firefly luciferase (FLuc) are easy to perform and that the results are generally highly reproducible.[27–29] To facilitate the analysis of protein biogenesis within the ER, we aimed to construct a FLuc-based reporter that manifests enzyme activity when cells experience defects in protein localization or disulfide bond formation within this organelle. To this end, we engineered FLuc based on the principles underlying the bacterial MalF-LacZ reporter's ability to detect such defects.[9,13]

Our results show that the new reporters are extremely sensitive in detecting abnormalities in these processes and that the results obtained are highly reproducible. In fact, the reporter system enabled us to reveal the strong impacts of altering the expression level of LMF1[25] and modulating the Ero1α[8] activity on the redox environment of the ER in mammalian cells. Furthermore, we demonstrated that the reporter can be customized to detect a protein translocation defect induced by a small molecule that inhibits the biosynthesis of a virus receptor.[30] Thus, this reporter system will serve as a valuable tool across various fields related to secretory pathway proteins.

RESULTS

Engineering FLuc for detecting a disulfide bond formation defect in the ER

To develop a convenient and sensitive reporter for identifying defects in disulfide bond formation or ER localization, we have adopted the principles underlying the bacterial MalF-LacZ reporter's ability to detect such defects (Figure S1). Consequently, we envisaged that it would function as a sensitive reporter of abnormalities in these processes if the reporter protein remained enzymatically active in the cytosol but becomes inactive upon localization to the ER due to disulfide bond formation (Figure 1Ai). To construct such a reporter, we used FLuc of *Photinus pyralis* as a reporter enzyme for reasons: Firstly, this FLuc is active in the cytosol. Secondly, the implementation of a "dual luciferase assay" using *Renilla* luciferase (RLuc) as an internal control (Figure 1Aii) greatly reduces experimental errors originating from variation in growth and transfection efficiency.[31] Accordingly, to identify defects in disulfide bond formation or ER localization, we use two different luciferase constructs that can be differently assayed. One (FLuc variant) is engineered to misfold in the oxidizing environment of the ER (Figure 1Ai), but the other (RLuc) is not (Figure 1Aii). The latter serves as an internal control. Thirdly, the assay is simple as it is performed by sequentially measuring luminescence after mixing the sample with ATP, Mg^{2+}, O_2, and a substrate for FLuc (D-luciferin), and then with O_2 and a substrate for RLuc (coelenterazine) within a single test tube, usually yielding the results in less than a minute. Finally, unlike GFP-based reporters, bioluminescence from luciferase does not necessitate excitation light. Thus, there is almost no autofluorescence generated, and thus background signals are generally negligible, leading to a high signal-to-noise ratio.[32,33] Probably, these advantageous properties contribute to the generally high reproducibility of results.[31] Consequently, FLuc has been effectively employed as an enzyme for various reporting purposes, including gene expression analysis, cell tracking, protein-protein interaction analysis, and assessment of cellular proteostasis status.[27–29]

As an initial step toward constructing the FLuc-based reporter, we adopted a plasmid expressing an ER-localized FLuc in which a 17-amino acid residue signal sequence of calreticulin (Calr, 17 aa) and a KDEL ER retrieval signal were fused to the N and C termini of FLuc of *P. pyralis*, respectively.[35] This FLuc has an N-glycosylation motif at Asn197, which undergoes "partial" N-glycosylation upon translocation into the ER.[35] We eliminated this ambiguity by mutating Asn197 to Gln (Figure 1Bii).

For this ER-localized FLuc to effectively serve as a sensitive reporter like bacterial MalF-LacZ, it should be strongly deactivated through disulfide bond formation (Figure 1A) (FLuc of *P. pyralis* has 4 cysteines [Figure 1C]). To test if this is the case, HeLa cells expressing the ER-localized FLuc were cultured for 2 h with or without 1 mM dithiothreitol (DTT), a reductant that breaks disulfide bonds in proteins, and the cell lysates were subjected to luciferase assay. Notably, the plasmid expressing FLuc was always co-transfected with a plasmid expressing RLuc, and FLuc activity was normalized against RLuc. Treatment with DTT resulted in a 2-fold increase in FLuc activity (Figure 1D), suggesting that disulfide bond formation mildly inhibited FLuc folding in the ER.

In contrast to β-galactosidase that possesses 16 cysteines,[9] FLuc of *P. pyralis* has only 4 cysteines (Figure 1C). Thus, to improve the sensitivity of the ER-localized FLuc as a reporter for ER disulfide bond formation deficiencies, we introduced cysteine substitutions to induce misfolding through disulfide bond formation. This change may allow sensitive detection of defects in disulfide bond formation, since the defects will lead to increased FLuc activity. Importantly, these cysteine substitutions should not adversely affect the enzyme activity when cysteine is in a reduced state. To find suitable residues for cysteine substitutions, we employed a consensus sequence-driven approach.[36] By analyzing multiple sequence alignments of FLucs and related enzymes, we identified positions where cysteine substitutions may be compatible with activity (Figure 1C). Indeed, cysteine substitutions at some of these positions only marginally affected the activity of "cytosolic FLuc" (Figure 1E, green). Therefore, we incorporated eight of the substitutions into the ER-localized FLuc to induce misfolding via disulfide bond formation (Figure 1Biii), yielding a variant containing a total of 12 cysteines (4 endogenous and 8 introduced cysteines). While incorporating these substitutions into the ER-localized FLuc led to a substantial reduction in luciferase activity (Figure 1F), inhibiting disulfide bond formation by

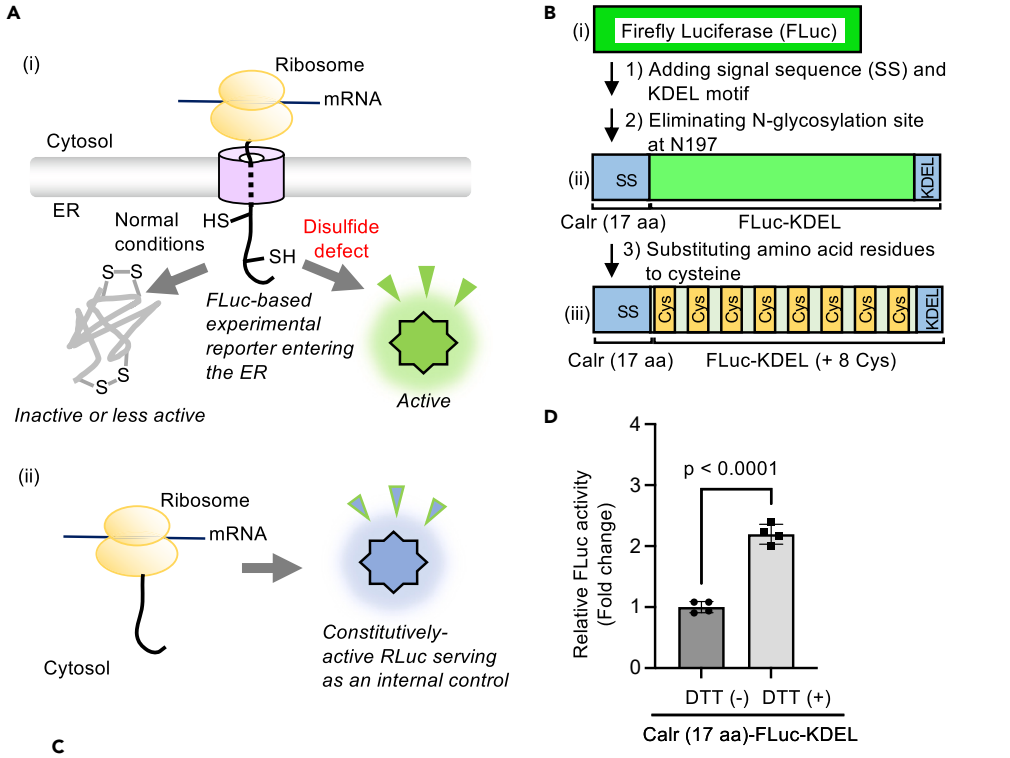

C

Species name	Residue in *P. pyralis* luciferase															
	C81	C216	C258	C391	V61	S85	L93	L115	V128	I145	S163	A222	I282	S314	V362	N463
Phrixothrix viviani	C	T	V	C	C	N	L	T	S	F	C	S	I	T	T	S
Phrixothrix hirtus	C	T	V	C	C	N	I	I	C	F	C	S	I	C	I	N
Luciola mingrelica	C	V	C	C	C	C	L	N	S	C	C	A	C	S	S	N
Hotaria parvula	C	V	C	C	C	C	L	N	S	C	C	A	C	S	S	N
Lampyroidea maculata	C	V	C	C	C	C	L	N	S	C	C	A	C	S	S	D
Luciola cruciata	C	V	C	C	C	C	I	V	S	T	C	A	C	S	S	S
Lampyris noctiluca	C	C	C	C	C	S	C	Y	C	I	S	C	I	S	C	F
Lampyris turkestanicus	C	C	C	C	C	S	C	Y	C	I	S	C	I	S	C	F
Pyrocoelia miyako	C	C	C	C	C	S	C	Y	C	V	S	C	I	S	C	F
Pyrocoelia rufa	C	C	C	C	C	S	C	Y	C	V	S	C	I	S	C	F
Cratomorphus distinctus	C	C	C	Y	C	S	C	Y	C	V	S	C	I	S	C	F
Photinus pyralis	**C**	**C**	**C**	**C**	**V**	**S**	**L**	**L**	**V**	**I**	**S**	**A**	**I**	**S**	**V**	**N**
Photuris pennsylvanica	C	V	C	Y	C	G	I	I	C	Y	C	C	V	S	T	Y
Pyrophorus plagiophthalamus	C	C	V	C	C	N	I	C	C	F	S	A	V	C	L	C
Pyrophorus mellifluus	C	C	V	C	C	N	I	C	C	F	S	A	V	C	L	C
Pyrearinus termitilluminans	C	C	V	C	V	N	I	C	T	Y	S	A	V	C	L	G
*Agrypnus binodulus**	C	S	S	C	C	N	C	V	C	F	C	A	V	C	S	C
Number of cysteines	17	9	11	15	15	4	6	3	10	3	8	6	4	5	5	3

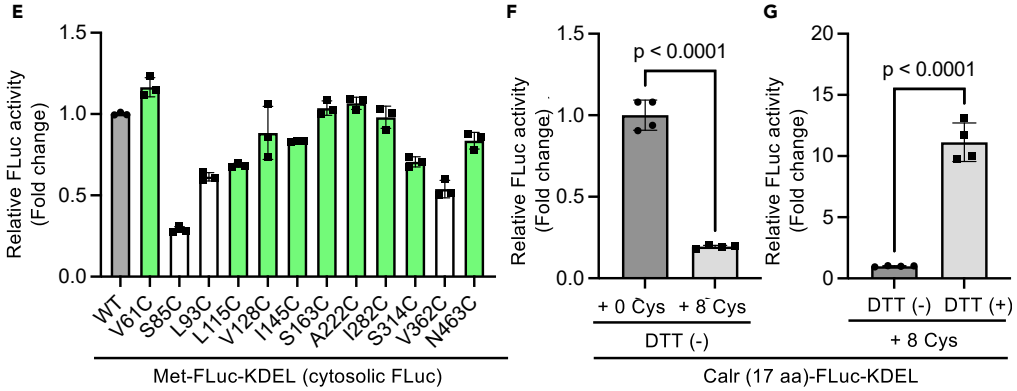

Figure 1. Engineering FLuc for detecting a disulfide bond formation defect in the ER

(A) (i) Rationale for detecting a disulfide bond formation detect in the ER using a prospective. FLuc-based reporter. (ii) *Renilla* luciferase (RLuc) serves as an internal control.

(B) Development of a FLuc-based reporter.

(C) Cysteine residues in FLucs and their close homologs. See Table S1 for the sources of amino acid sequences aligned using ClustalW. Residue numbers correspond to *P. pyralis* FLuc. Cysteines occurring more than twice at each position are listed. Proteins from Phengodidae (glowworm), Lampyridae (firefly), and Elateridae (click beetle) families are denoted in blue, black, and magenta, respectively. They belong to insect luciferases except for *Agrypnus binodulus* fatty acyl-CoA synthetase (*asterisk*).[34].

(D) Effect of DTT treatment on FLuc activity in cells expressing Calr (17 aa)-FLuc-KDEL. HeLa cells, cultured in 6-well plates, were transfected with 95 ng of a plasmid expressing Calr (17 aa)-FLuc-KDEL and 5 ng of pRL-SV40 expressing RLuc. After 24 h, cells lysates were subjected to a dual luciferase assay. Where indicated, 1 mM DTT was added to the culture 2 h before harvest. The data represent the means ± SD from four independent samples. Statistical analysis utilized a two-tailed Student's t test. *p* values are indicated in the graph.

(E) Effects of cysteine substitutions on the activity of FLuc produced in the cytosol. HeLa cells, grown in 6-well plates, were transfected with 380 ng of a plasmid expressing the indicated FLuc variant in the cytosol, and 20 ng of pRL-SV40. After 24 h, cell lysates were subjected to a dual luciferase assay. The data represent the means ± SD from three independent samples.

(F) Effect of introducing eight cysteine substitutions (V61C, L115C, V128C, S163C, A222C, I282C, S314C, and N463C) into Calr (17 aa)-FLuc-KDEL on Fluc activity.

(G) Effect of DTT treatment on FLuc activity in cells expressing Calr (17 aa)-FLuc-KDEL with eight cysteine substitutions. Where indicated, 1 mM DTT was added to the culture 2 h before harvest. In (F) and (G), the data represent the means ± SD from four independent samples. Statistical analysis was performed as described in (D).

treatment with 1 mM DTT effectively restored the enzyme activity (Figure 1G). Thus, the cysteine substitutions enabled the creation of an ER-localized FLuc that can detect disulfide bond formation deficiencies in this organelle.

Reporter sensitivity is greatly improved by enhancing the ER translocation of FLuc*

Next, the luciferase portion of the reporter was linked with a triple FLAG tag (FLAG) for detection purposes and with tandemly duplicated N-glycosylation sites (N-gly) to investigate its ER translocation.[37] The resulting luciferase portion was denoted as FLuc*, and the full-length protein as Calr (17 aa)-FLuc* (Figure 2Aiv). Importantly, the addition of these supplementary sequences did not alter the reporter's fundamental capacity to detect ER disulfide bond formation defects (Figure 2B).

Notably, in the lysates of HeLa cells expressing the reporter, we detected two bands using an anti-FLAG antibody (Figure 2C, lane 3). We suggest that the lower band (indicated by open arrowhead) represents the reporter protein that failed to enter the ER, as only the upper band was susceptible to endoglycosidase H (Endo H) treatment (Figure 2C, lanes 3 and 4). Since the cytosol is a reducing environment, the reporter protein that fails to enter the ER would fold into its active enzyme in the cytosol. Thus, mis-localization of FLuc* to the cytosol would unfavorably elevate the background activity, leading to reduced sensitivity of the reporter for ER disulfide bond formation defects.

To enhance the translocation of FLuc* into the ER, we utilized that the early mature regions of secreted proteins often facilitate protein secretion.[38] We, thus, constructed a reporter in which FLuc* is fused with the N-terminal 40 residues of calreticulin, including its signal peptide and the initial 23 amino acids of the mature protein. This fused protein was designated as Calr (40 aa)-FLuc* (Figure 2A-v). While fusion of the longer N-terminal sequence led to a significant reduction in FLuc activity (Figure 2D), inhibiting disulfide bond formation by DTT treatment greatly elevated FLuc activity compared to non-treated cells (Figure 2E). Importantly, DTT treatment did not alter the ER localization of FLuc* (Figure S2). Thus, fusion of the longer N-terminal sequence to FLuc* rendered the reporter more sensitive to ER disulfide bond formation defects.

Detection of a protein targeting defect using a simple enzyme assay

Treating cells expressing Calr (40 aa)-FLuc* with 1 mM DTT greatly elevated FLuc activity (Figure 2E), suggesting that FLuc* was inactivated via disulfide bond formation in the ER (see also Figure 5C, lane 5). Consistently, the majorities of FLuc* formed disulfide-linked oligomers in cells expressing Calr (40 aa)-FLuc* under normal conditions (data not shown). In contrast, the cytosol is a reducing environment. Thus, inhibiting FLuc* targeting to the ER would also enable it to attain enzymatically active conformation within the cytosol. In fact, deleting the signal sequence-containing N-terminal sequence from Calr (40 aa)-FLuc* generated a constitutively active reporter that is insensitive to DTT treatment (Figure S3). Therefore, protein localization deficiencies may also be detected as an increase in FLuc activity using a FLuc* reporter.

To validate this, we investigated the response of a FLuc* reporter to a protein targeting deficiency caused by knockdown of SRP54, an essential component of the signal recognition particle (SRP) required for ER protein targeting.[2] To test the applicability of the FLuc* system to other ER signal sequence, we employed the signal sequence-containing N-terminal 40 amino acids of the human interleukin-6 receptor alpha subunit (IL6R) (Figure 3A). SRP54 knockdown (Figure 3B, lanes 2 and 3) led to the accumulation of a fraction of FLuc* that failed to enter the ER (Figure 3C, lanes 3 and 5, open arrowheads), resulting in significant elevation of FLuc activity (Figure 3D, Rescue (−)). This response was not due to small interfering RNA (siRNA) off-target effects, as expression of siRNA-resistant SRP54 in knockdown cells (Figure 3B, lanes 5 and 6; Figure 3E, lanes 3 and 5) significantly lowered the FLuc activity (Figure 3D, Rescue (+)). Thus, the FLuc* fusion protein serves as a convenient and sensitive reporter for detecting protein targeting deficiencies induced by SRP54 knockdown.

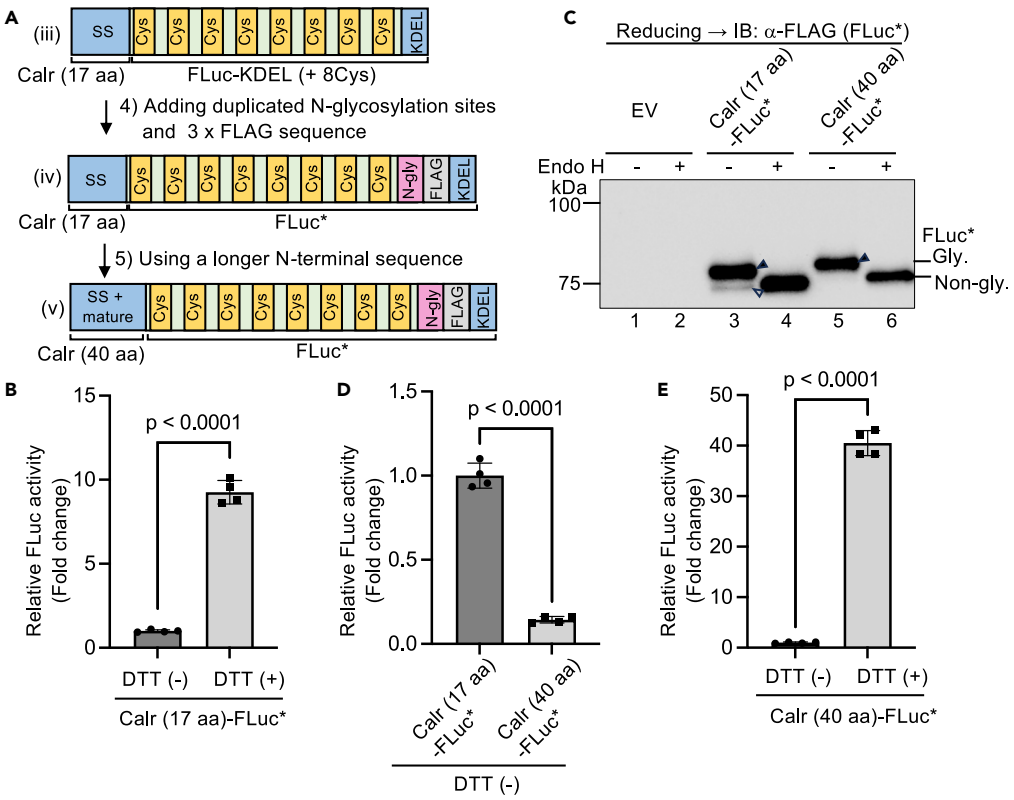

Figure 2. Reporter sensitivity is greatly improved by enhancing the ER translocation of FLuc*

(A) Modifications implemented in the reporter.

(B) Effect of incorporating tandemly duplicated N-glycosylation sites and a triple FLAG tag on the reporter's response. HeLa cells expressing Calr (17 aa)-FLuc* were cultured, treated with or without 1 mM DTT for 2 h, lysed, and subjected to a dual luciferase assay.

(C) Detection of the reporter proteins in HeLa cells (6.0 μg) expressing Calr (17 aa)-FLuc* or Calr (40 aa)-FLuc*. Where indicated, lysates were treated with endoglycosidase H (Endo H) to identify the glycosylated (*Gly.*), and non-glycosylated (*Non-gly.*) forms of FLuc*. Closed arrowheads, glycosylated FLuc*; open arrowhead, non-glycosylated FLuc*.

(D) Effect of inserting the early mature region of calreticulin on FLuc activity. HeLa cells expressing either Calr (17 aa)-FLuc* or Calr (40 aa)-FLuc* were lysed and subjected to a dual luciferase assay.

(E) Effect of DTT treatment on FLuc activity of HeLa cells expressing Calr (40 aa)-FLuc*. Where indicated, 1 mM DTT was added to the culture 2 h before harvest. In (B–E), the data represent the means ± SD from four independent samples. Statistical analysis was performed using a two-tailed Student's t test.

Creating an assay to evaluate the ability of a small molecule to inhibit virus receptor biosynthesis

Signal sequences play essential roles in the targeting and translocation of numerous proteins into the ER. Yet, they have diverse and unique amino acid sequences.[39] Thus, a small molecule recognizing the signal sequence of a disease-associated protein holds potential as a drug since it may inhibit its biosynthesis. For instance, cyclotriazadisulfonamide (CADA) (Figure 4A) binds to the signal sequence of human CD4, a receptor for human immunodeficiency virus (HIV) and thereby prevents its biosynthesis (translocation across the ER membrane) (Figure 4B), resulting in the inhibition of HIV entry into T cells.[30]

Although novel small-molecule inhibitors of protein localization may contribute to medicine, developing high-throughput screening assays for them is generally difficult.[40] Consequently, we examined whether our reporter system can identify a protein translocation deficiency caused by CADA.[30] To this end, we fused the signal sequence-containing N-terminal 40 amino acid residues of human CD4 to FLuc* (Figure 4C). Remarkably, exposure of HeLa cells expressing the reporter with 2 μM CADA for 4 h resulted in a marked increase in FLuc activity (Figure 4D), accompanied by accumulation of the non-glycosylated form of FLuc* (Figure 4E, lane 2, open arrowhead). Notably, this response was not observed with the negative control reporter, bPRL (40 aa)-FLuc*, carrying a CADA-insensitive signal sequence from the bovine preprolactin precursor[30] (Figures 4F and 4E, lanes 5–8). Thus, the FLuc* reporter system can effectively identify a protein translocation defect induced by a small molecule.

Inhibiting Ero1α-dependent oxidation of PDI has a direct impact on the redox environment of the ER

In eukaryotic cells, members of the protein disulfide isomerase (PDI) family introduce disulfide bonds into their target proteins (substrates) in the ER, which require reoxidation to undergo another catalytic cycle. This reoxidation is facilitated by enzymes known as PDI oxidases. In

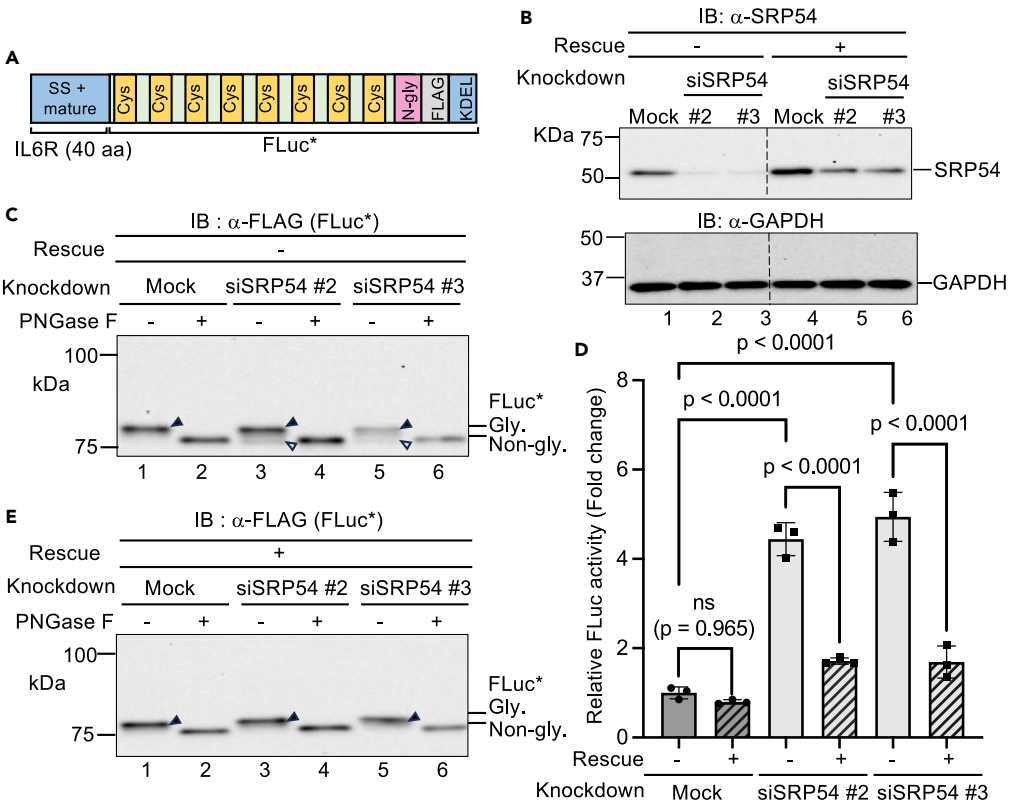

Figure 3. Detection of a protein targeting defect using a simple enzyme assay

(A) Structure of IL6R (40 aa)-FLuc*.

(B) Confirmation of siRNA-mediated knockdown of SRP54. HeLa cells, cultured in 6-well plate, were transfected with 20 nM of either a control siRNA (*Mock*), or SRP54-specific siRNAs #2, or #3 using Lipofectamine RNAiMAX. After 24 h, cells were further transfected with 95 ng of a plasmid expressing ILR6R (40 aa)-FLuc*, 5 ng of pSV40-RLuc, and 100 ng of an empty vector (pcDNA3.1^{+}) (*Knockdown*) or a rescue plasmid expressing siRNA-resistant SRP54 (*Rescue*) using Effectene. After additional 24 h, cell lysates (3.5 μg) were subjected to reducing SDS-PAGE, and immunoblotting with an antibody against SRP54 (*upper*) or GAPDH (*lower*) for knockdown confirmation.

(C and E) Detection of the reporter protein in cell lysates (4.0 μg) obtained as described in (B). Cell lysates were treated with or without Peptide -*N*-Glycosidase F (PNGase F) to identify the glycosylated (*Gly.*) and non-glycosylated (*Non-gly.*) forms of FLuc*. Closed arrowheads, glycosylated FLuc*; open arrowheads, non-glycosylated FLuc*. Note that SRP54 knockdown resulted in the accumulation of FLuc* that failed to enter the ER (open arrowheads in C). This protein export defect was rescued by co-transfection of a plasmid expressing siRNA-resistant SRP54 as indicated by the disappearance of the non-glycosylated form (E).

(D) Effect of SRP54 knockdown on FLuc activity in cells expressing ILR6R (40 aa)-FLuc* (see B for the knockdown experiments). The data represent the means ± SD from three independent samples. Statistical analysis utilized one-way ANOVA followed by Tukey's test. "ns" denotes not significant ($p > 0.05$).

mammalian cells, multiple PDI oxidases exist, each with distinct specificities toward PDI family members. These include endoplasmic reticulum oxidoreductase 1 alpha (Ero1α), endoplasmic reticulum oxidoreductase 1 beta (Ero1β), peroxiredoxin 4 (Prx4), and glutathione peroxidase 7 (GPx7).[8,41,42] Among them, Ero1α is presumed to play a central role in disulfide bond formation pathway by oxidizing PDI, a canonical PDI family member[8] (Figure 5A, right). However, the detection of Ero1α activity using ER-localized roGFP variants in mammalian cells is notoriously challenging and often necessitates repeated measurements to ensure data reliability[26] or a "DTT pulse experiment." In the latter experiment, cells expressing an ER-localized roGFP variant are initially treated with a low concentration of DTT to reduce cellular proteins. After removing DTT from the medium, the recovery of the oxidative conditions of the ER is monitored by measuring the redox-dependent change in fluorescence properties of the ER-localized roGFP variant.[22,23] It is thought that these steps are necessary as multiple mechanisms operate to preserve the capacity for disulfide bond formation in the ER of mammalian cells.[23]

Here, we examined the impact of inhibiting Ero1α-dependent oxidation of PDI on the ER's redox environment using the reporter system. Given the redundancy in mechanisms preserving the capacity for disulfide bond formation in the ER (see earlier text), we deemed genetic ablation of Ero1α impractical. Thus, we employed a chemical inhibitor to acutely disrupt Ero1α activity. For this purpose, we utilized bisphenol A (BPA) (Figure 5A, left), an inhibitor of Ero1α-catalyzed PDI oxidation with a 50% inhibitory concentration (IC_{50}) of 41 μM. This compound rapidly inhibits PDI reoxidation in HeLa cells, resulting in the accumulation of a substantial amount of PDI in its reduced form.[43] Upon treatment of HeLa cells expressing Calr (40 aa)-FLuc* with BPA, we observed a dose-dependent elevation in FLuc activity (Figure 5B). This suggests that inhibiting Ero1α-dependent oxidation of PDI alters the ER's redox environment, despite the presence of redundant pathways for disulfide

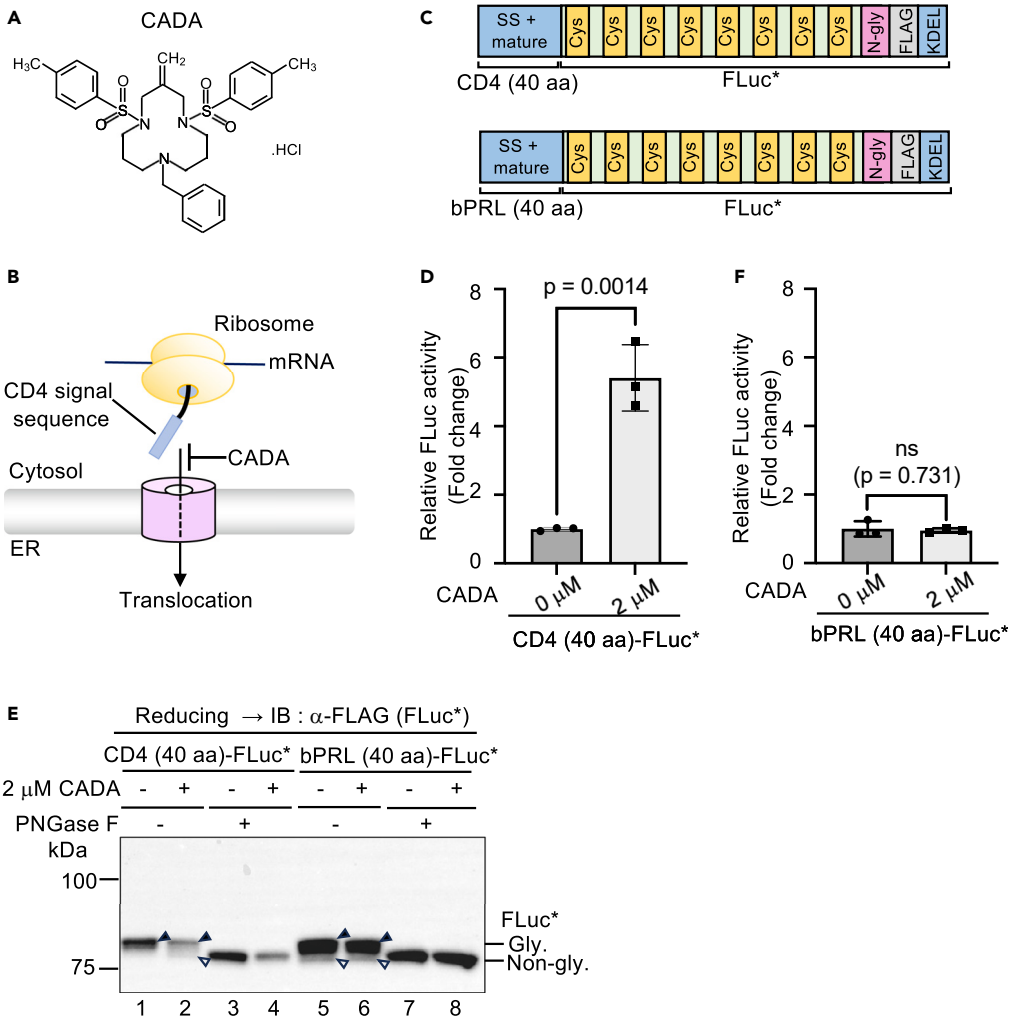

Figure 4. Creating an assay to evaluate the ability of a small molecule to inhibit virus receptor biosynthesis

(A) Structure of CADA.[30].

(B) CADA binds to the signal sequence of human CD4, leading to the inhibition of CD4 biosynthesis.[30].

(C) Structures of FLuc* reporters, CD4 (40 aa)-FLuc* and bPRL (40 aa)-FLuc*.

(D) Effect of CADA treatment on FLuc activity of HeLa cells expressing CD4 (40 aa)-FLuc*. HeLa cells were cultured in 6-well plates, transfected with 38 ng of a plasmid expressing CD4 (40 aa)-FLuc* and 2 ng of pSV40-RLuc. After 20 h, cells were treated with or without 2 μM CADA for 4 h, lysed, and subjected to a dual luciferase assay.

(E) Effect of CADA treatment on the localization of CD4 (40 aa)-FLuc* or bPRL (40 aa)-FLuc*. Cells lysates (7.5 μg) obtained as described in (D) and (F) were treated with or without PNGase F and subjected to reducing SDS-PAGE and immunoblotting with anti-FLAG antibody to identify the glycosylated (*Gly.*) and non-glycosylated (*Non-gly.*) forms of FLuc*. Closed arrowheads, glycosylated FLuc*; open arrowheads, non-glycosylated FLuc*.

(F) Effects of CADA treatment on FLuc activity of bPRL (40 aa)-FLuc* expressed in HeLa cells. The experiments were conducted as described in (D), except that bPRL (40 aa)-FLuc* was used as an FLuc* reporter. In (D) and (F), the data represent the means ± SD from three independent samples. Statistical analysis was performed using a two-tailed Student's t test.

bond formation.[23] We next investigated the effect of the BPA treatment on the oxidative state of FLuc* (which contains a total of 12 cysteines) using maleimidyl polyethylene glycol 2000 (Mal-PEG 2000), a reagent that specifically reacts with free cysteines and retards the mobility of proteins on gels. In mock-treated cells, FLuc* displayed smeared bands between fully oxidized (FLuc* without Mal-PEG) and fully reduced FLuc* (Figure 5C, lane 5), consistent with that introducing cysteine substitutions into the ER-localized FLuc impaired the enzyme activity via disulfide bond formation (Figure 2E). Remarkably, treating the cell culture with BPA resulted in the appearance of a fraction of FLuc* at the fully reduced position (Figure 5C, lane 4, asterisk), consistent with the observed increase in FLuc activity (Figure 5B). This treatment did not change the ER localization of FLuc* (Figure S4). Thus, despite the redundancy of pathways for disulfide bond formation,[23] inhibiting Ero1α-dependent oxidation of PDI alters the ER's redox environment. This change can be detected using a simple FLuc assay, highlighting the convenience of the reporter system.

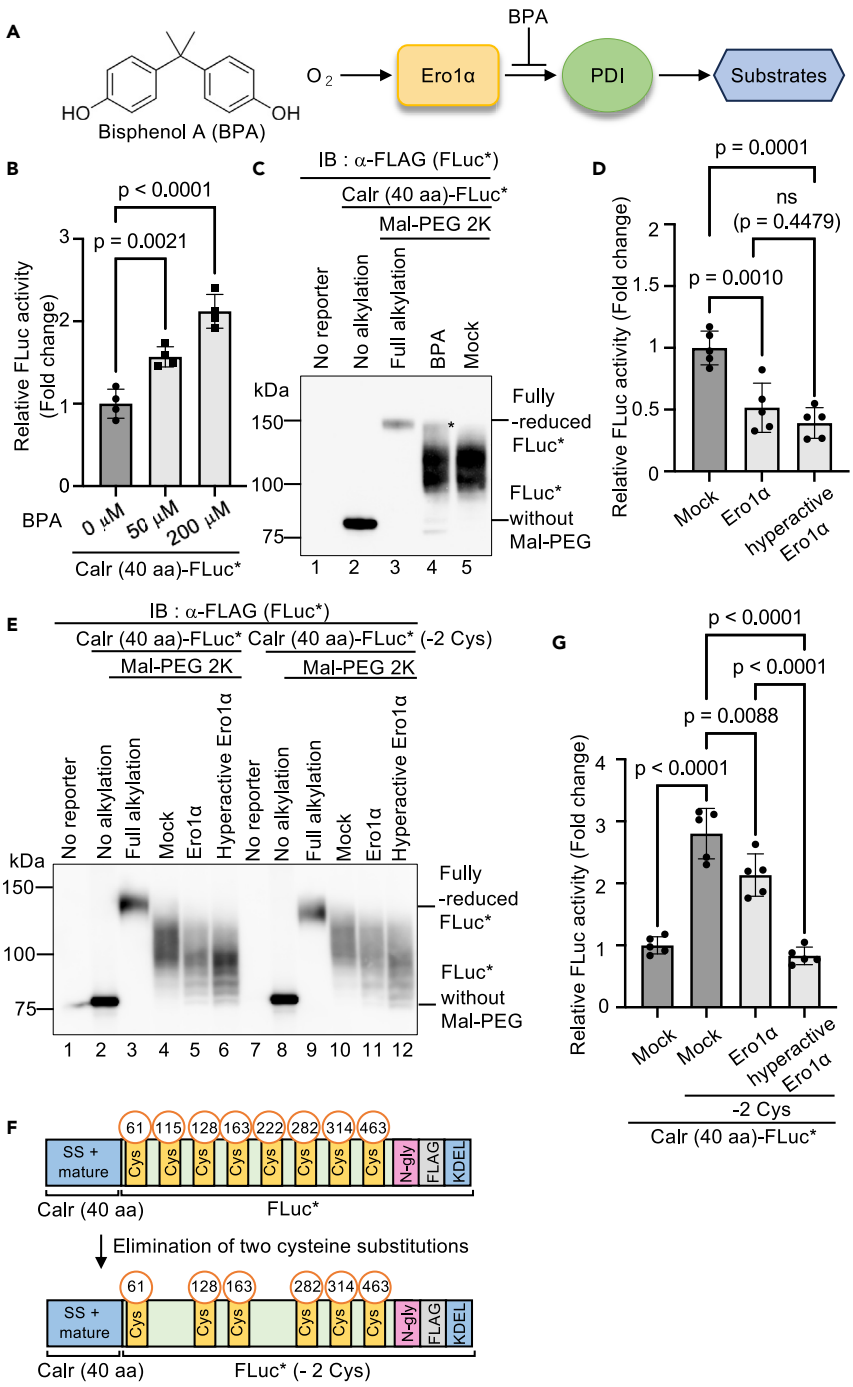

Figure 5. Modulating the Ero1α activity has significant impacts on the redox environment of the ER

(A) Structure of Bisphenol A (BPA) (*left*), an inhibitor of the Ero1α-dependent oxidation of PDI (*right*).[43]

(B) Effect of BPA treatment on FLuc activity of HeLa cells expressing Calr (40 aa)-FLuc*. Before assay, the cultures were treated with the indicated concentrations of BPA for 2.5 h. The data represent the means ± SD from four independent samples. One-way ANOVA followed by Dunnett's test was used for statistical analysis.

(C) Effect of BPA treatment on the oxidative state of FLuc*. HeLa cells expressing Calr (40 aa)-FLuc* were treated with (*BPA*) or without (*Mock*) 200 μM BPA for 2.5 h, subjected to alkylation with Mal-PEG 2000 (*Mal-PEG 2K*), separated by reducing SDS-PAGE, and detected with anti-FLAG antibody. Lane 1, mock-transfected cells. Lane 2, no alkylation. Lane 3, proteins fully reduced in a buffer (100 mM Tris-HCl [pH 8.0], 100 mM DTT and 1% SDS) before alkylation of free cysteines with Mal-PEG 2000. An asterisk on lane 4 indicates the fully reduced form of FLuc* appearing upon treatment of cells with BPA.

(D) Effect of overexpressing Ero1α and its hyperactive mutant on FLuc activity of HeLa cells expressing Calr (40 aa)-FLuc*.

(E) Effect of overexpressing Ero1α or its hyperactive mutant on the oxidative states of indicated FLuc* reporter proteins assessed as described in panel C.

Figure 5. *Continued*

(F) Structures of Calr (40 aa)-FLuc* and Calr (40 aa)-FLuc* (−2 Cys) reporters.

(G) Effect of overexpressing Ero1α and its hyperactive mutant on FLuc activity of HeLa cells expressing Calr (40 aa)-FLuc* (−2 Cys). For comparison, the activities were normalized with that of cells expressing Calr (40 aa)-FLuc*. In (D) and (G), the data represent the means ± SD from five independent samples. Statistical analysis utilized one-way ANOVA followed by Tukey's test.

Tailoring FLuc* for sensitive detection of increases in disulfide bond formation capacity

We then assessed if the FLuc* reporter could detect ER alternation resulting from Ero1α overexpression. Upon Ero1α overexpression, we observed the diminished FLuc activity (Figure 5D) and enhanced oxidation of FLuc*, as demonstrated by its increased mobility on SDS-PAGE (Figure 5E, lanes 4 and 5). Moreover, overexpression of Ero1α or its hyperactive mutant (see in the following) did not alter the ER localization of FLuc* (Figure S5). Thus, the FLuc* reporter can detect ER oxidation induced by Ero1α overexpression.

Ero1α is thought to undergo feedback regulation to prevent ER hyper-oxidation in a process dependent on Cys104 and Cys131. Mutating these cysteines generates a constitutively active Ero1α.[44–46] To examine if these mutations affect the disulfide bond formation capacity of the ER, we overexpressed the hyperactive mutant of Ero1α in HeLa cells carrying the Calr (40 aa)-FLuc* reporter. However, no statistically significant difference was observed in FLuc activity between cells overexpressing the wild-type Ero1α and those overexpressing the hyperactive mutant of Ero1α (Figure 5D). Thus, discriminating between these two conditions seems difficult with the reporter assay, suggesting that nearly all ER-localized FLuc* molecules were inactivated by disulfide bond formation under these conditions (Figure 5E, lanes 4–6).

Accordingly, we considered that raising the basal luciferase activity by reducing the number of cysteine substitutions in FLuc* might enhance the reporter's ability to detect a wider range of "increases" in disulfide bond formation capacity. Consequently, we removed two cysteine substitutions from Calr (40 aa)-FLuc* to construct a reporter named "Calr (40 aa)-FLuc*(-2 Cys)" (Figure 5F). As expected, the basal luciferase activity increased with the new reporter (Figure 5G, Mock, −2 Cys). Remarkably, this reporter allowed us to detect changes in disulfide bond formation capacity resulting from the introduction of hyperactive mutations into Ero1α (Figures 5G and 5E, lanes 10–12). Thus, by reducing the number of cysteine substitutions in FLuc*, we successfully constructed a reporter that is more suited for detecting increases in disulfide bond formation capacity of the ER.

These findings indicate that modulation of the Ero1α activity, by either a specific inhibitor of Ero1α-dependent oxidation of PDI or mutating a regulatory cysteine pair, does alter the redox environment of the ER toward a more reducing or oxidizing state. Furthermore, we effectively identified these changes simply by measuring FLuc activity in cell lysates, emphasizing the exceptional convenience of the reporter system.

LMF1 participates in the redox control of the ER

In a protein with three or more cysteines, two cysteines can be joined in a disulfide bond that does not appear in the native structure. Such nonnative disulfide bonds can indeed be transiently formed during the biosynthesis of secretory pathway proteins in various organisms.[6,16,47] It is thought that the supply of reducing equivalents (electrons) to the site of oxidative folding is essential for efficiently breaking and repairing nonnative disulfide bonds in proteins.[16,48,49] Notably, Roberts et al.[25] showed that the absence of an ER membrane protein, LMF1, leads to a more oxidizing ER and that this protein is required for the folding of certain proteins requiring the reduction of nonnative disulfide bonds during their folding. Their findings led to the proposal that LMF1 affects ER redox homeostasis by directly or indirectly providing reducing equivalents (electrons) to this compartment[25] (Figure 6A). However, using an roGFP reporter, Roberts et al.[25] could detect significant alterations to the redox environment upon LMF1 overexpression only in cells also expressing a disulfide-rich, ER client protein, lipoprotein lipase (LPL).

If LMF1 participates in providing electrons to the ER, and FLuc* can receive these electrons, disulfide bonds in FLuc* would be cleaved, leading to the activation of FLuc*. To test this, we overexpressed or silenced LMF1 in HeLa cells carrying the Calr (40 aa)-FLuc* reporter. While LMF1 overexpression greatly elevated FLuc activity (Figure 6B), silencing LMF1 significantly lowered the activity (Figure 6C, LMF1-KD), consistent with that LMF1 supplies electrons to the ER. Importantly, expression of a silencing-resistant LMF1 variant in the silenced cells restored FLuc activity (Figure 6C, Rescue) (see also Figure S6). Furthermore, LMF1-overexpression-mediated increase in FLuc activity was accompanied by disulfide bond cleavage in FLuc* (Figure 6D, lane 5). Importantly, the changes in FLuc activity were not caused by mis-localization of FLuc* to the cytosol, as FLuc* remained fully N-glycosylated under the conditions (Figure 6E, lanes 3 and 5; Figure S7). Thus, alteration of LMF1 levels significantly influenced the ER's redox environment. These findings are consistent with the proposal that LMF1 participates in the redox control of the ER by directly or indirectly providing reducing equivalents to this compartment.[25]

Notably, Roberts et al.[25] measured multiple cells per condition to assess the effects of LMF1 overexpression or knockdown using ERroGFP-S4, a roGFP derivative optimized for measuring the redox environment in the ER. Yet, they could only detect effect of LMF1 overexpression on the redox environment in cells also expressing LPL. By contrast, our measurements with FLuc* showed an over 10-fold increase in activity upon LMF1 overexpression in unstressed cells, and a ∼50% decrease in activity upon LMF1 knockdown. These findings underscore the high sensitivity and reproducibility of the FLuc* reporter assay for evaluating changes to the ER redox environment.

DISCUSSION

Approximately 30% of the human proteome enters the ER and undergoes disulfide bond formation to facilitate proper folding and functionality. Consequently, understanding the mechanisms governing these processes is highly important. Here, we describe the successful

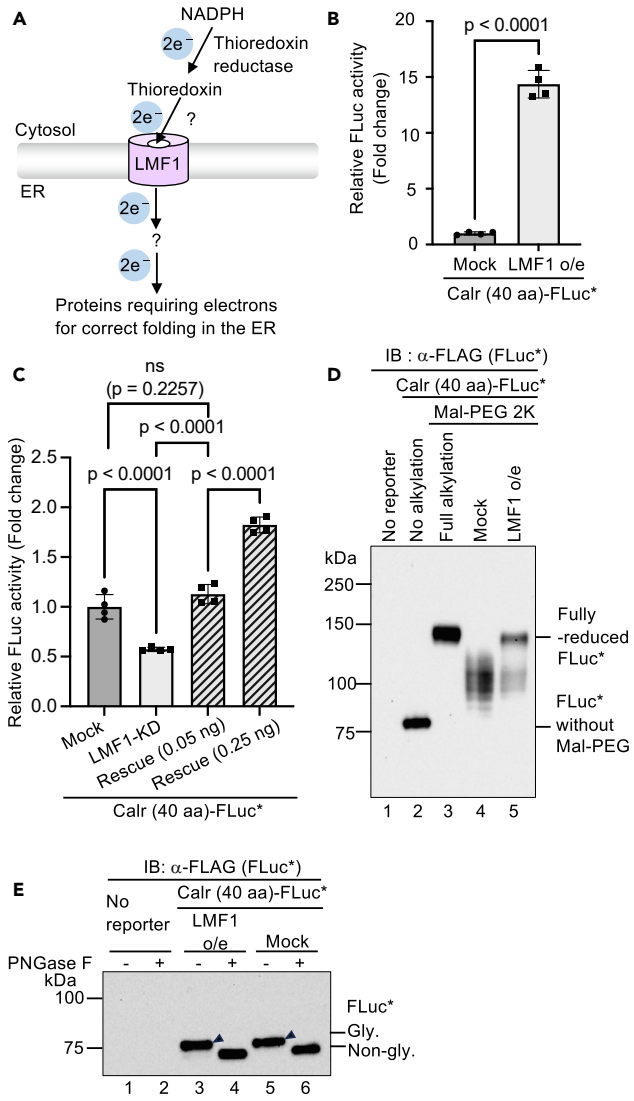

Figure 6. LMF1 participates in the redox control of the ER

(A) Model illustrating the putative function of LMF1.

(B) Effect of overexpressing LMF1 on FLuc activity of HeLa cells expressing Calr (40 aa)-FLuc*. The data represent means ± SD from four independent samples. Statistical analysis was performed using a two-tailed Student's t test.

(C) Effect of siRNA-mediated knockdown of LMF1 on FLuc activity of HeLa cells expressing Calr (40 aa)-FLuc*. HeLa cells were initially transfected with 20 nM of control (*Mock*) or LMF1-specific siRNA (*LMF1-KD*) using Lipofectamine RNAiMAX and grown in 6-well plates. After 24 h, cells were transfected with 38 ng of a plasmid expressing Calr (40 aa)-FLuc*, and 2 ng of pRL-SV40. Where indicated, LMF1-knockdown cells were co-transfected with an indicated amount of a plasmid expressing an siRNA-resistant PA-LMF1 (*Rescue*). After 24 h, cells lysates were subjected to a dual luciferase assay. The data represent the means ± SD from four independent samples. Statistical analysis utilized one-way ANOVA followed by Tukey's test. Note that PA-LMF1 is an LMF1 derivative fused with a PA tag (12 amino acid residues) at its N terminus for detection purposes. Expression of PA-LMF1 in the knockdown cells at levels comparable to endogenous LMF1 restored FLuc* activity (Figures 6 and S6), confirming that the decrease in FLuc* activity observed in LMF1-knockdown cells was not caused by secondary effects of the siRNA used.

(D) Effect of LMF1 overexpression on the oxidative states of FLuc* assessed using Mal-PEG 2000 (Mal-PEG 2K) as described in Figure 5C.

(E) Effect of LMF1 overexpression on the N-glycosylation status of the reporter protein assessed as described in Figure 3C and 3E.

development of a new reporter system capable of sensitively and reproducibly detecting abnormalities in these two crucial steps of secretory pathway protein biosynthesis, simply by measuring luciferase activity of the cell lysates.

The reporter system was developed by introducing cysteine substitutions into ER-localized FLuc. This approach was inspired by the rationale underlying bacterial MalF-LacZ and similar fusions used for detecting defects in bacterial cell envelope protein biogenesis.[9,13] Notably, similarly to other luciferase-based reporters, the developed system exhibited high sensitivity, reproducibility, and convenience in detecting defects in the processes (Figures 1, 2, 3, 4, 5, and 6).

It should be noted that failure to enter the ER or impaired disulfide bond formation can promote the enzyme activity. When it is necessary to distinguish between these two effects, it can be achieved by examining the localization of the probe (FLuc*) by N-glycosylation assay and/or its oxidative state by Mal-PEG alkylation assay as described (Figures 2C, 3C, 4E, 5C, 5E, 6D, and 6E).

We have constructed various FLuc-based reporters. While Calr (40 aa)-FLuc* can detect general defects in protein disulfide bond formation (Figures 2, 5, and 6), its variant lacking two cysteine substitutions, Calr (40 aa)-FLuc* (−2 Cys), is suitable for observing increases in disulfide bond formation capacity of the ER (Figure 5). Although we presented that IL6R (40 aa)-FLuc* can detect a protein translocation deficiency originating from SRP54 knockdown (Figure 3), any FLuc* fusions containing an efficient ER signal sequence will serve the same purpose. Furthermore, the reporter can be tailored to assess the protein localization capacity of a specific signal sequence by fusing the precursor protein's N-terminal sequence to FLuc* (Figure 4, and see in the following).

It is important to note that FLuc-based-reporters often lack dynamic readout (reversibility) due to their continued activity once properly folded.[29] Additionally, cell lysis is basically needed for the assay as FLuc relies on ATP, magnesium ions, oxygen, and D-luciferin substrate for luminescence.[32] Consequently, FLuc-based reporters, including our FLuc* reporters, are less suitable for a real-time, in-cell sensor, unlike fluorescent probes.[29]

Yet, despite their lack of dynamic readout, these reporters offer the advantage of accumulating a signal over extended periods, allowing discrimination of even subtle changes in the environment.[17] Furthermore, due to their lack of reversibility, assays can be conducted using pre-prepared cell lysates, contributing to the easiness of the measurement compared to real-time sensors susceptible to environmental fluctuations.[17]

These features of the reporter system, lacking in fluorescent reporters, enabled us to demonstrate that modulation of the Ero1α activity, by either a specific inhibitor of Ero1α-dependent oxidation of PDI or mutating a regulatory cysteine pair, does affect the ER's redox environment despite redundant pathways for disulfide bond formation[23] (Figure 5) and that LMF1 has a great impact on the redox environment of the ER[25] (Figure 6). Given the critical role of maintaining the proper redox environment for efficient oxidative protein folding,[8] these findings provide the basis for our understanding of the ER as the primary folding compartment for numerous secretory pathway proteins.

Here, we showed several lines of evidence that FLuc* reporters serve as sensitive, reproducible, and convenient probes of defects in ER protein translocation or protein disulfide bond formation (Figures 2, 3, 4, 5, and 6). Thus, the reporters will be invaluable for investigating factors or mechanisms related to critical steps in the biogenesis of numerous cell surface proteins, including studies on redox balance maintenance and protein translocation.

Importantly, the utility of the reporter system will extend beyond fundamental studies. Some cell surface proteins contribute to disease development, including those involved in virus entry into human cells,[50] and autoimmune diseases.[51] Here, we demonstrated that fusing the N-terminal sequence of an HIV receptor to FLuc* allowed easy evaluation of the ability of CADA, to hinder HIV receptor's signal sequence function (Figure 4). Given that luciferase-based assays are well-suited for high-throughput platforms,[31] we suggest that this approach will facilitate large-scale screening of small molecules that specifically block the biosynthesis of a harmful secretory pathway protein.

Limitations of the study

While our study supports the model by Roberts et al., which suggests that LMF1 influences ER redox homeostasis by directly or indirectly supplying reducing equivalents to this compartment,[25] many aspects of LMF1's function remain unclear. Further investigation is necessary to clarify the molecular function of LMF1.

RESOURCE AVAILABILITY

Lead contact

Further information and request for resources and reagents should be directed to and will be fulfilled by the lead contact, Hiroshi Kadokura (kadokura.h.3c47@m.isct.ac.jp).

Materials availability

All unique and stable reagents generated in this study are available from the lead contact upon request.

Data and code availability

- Data reported in this paper will be shared by the lead contact upon request.
- This paper does not report original code.
- Any additional information required to reanalyze the data reported in this paper is available from the lead contact upon request.

ACKNOWLEDGMENTS

We thank the current and former members of Inaba, Kohno, and Taguchi laboratories especially Yuichi Tsuchiya (RIKEN Center for Brain Science) for discussion and Satoshi Kanda (Graduate School of Medicine, Osaka University) for the gift of a mouse cDNA clone for SRP54.

This work was supported by JSPS KAKENHI grants JP22H02253, JP20K21262 (to H.K.), and 17H01468 (to K.K.); Japan Foundation for Applied Enzymology (to H.K.); Takeda Science Foundation (to K.K.); Ohsumi Frontier Science Foundation (to K.K.); and AMED-CREST under grant number JP21gm1410008 (to H.T.) and 21gm1410006h0001 (to K.I.). This work was partly supported by the Cooperative Research Project Program of the Medical Institute of Bioregulation, Kyushu University.

AUTHOR CONTRIBUTIONS

H.K. conceived the project, provided supervision, designed and performed experiments, analyzed data, and wrote the manuscript. N. Harada, S.Y., N. Hirai, and R.T. designed and performed reporter assays, cell experiments, and statistical analysis and prepared the figures. R.T. and K.A. prepared antibody to LMF1. Y.A. assisted in the statistical analyses and wrote the manuscript. D.N. designed experiments and provided plasmids. K.Y. designed experiments, analyzed data, and wrote the manuscript. H.T., K.K., and K.I. analyzed the data, provided supervision, and wrote the manuscript. All authors discussed the results and approved the manuscript.

DECLARATION OF INTERESTS

The authors declare no competing interests.

DECLARATION OF GENERATIVE AI AND AI-ASSISTED TECHNOLOGIES IN THE WRITING PROCESS

During the preparation of this work, the authors used ChatGPT-3.5, OpenAI, to improve language and readability. After using this service, the authors reviewed and edited the content as needed and take full responsibility for the content of publication.

STAR★METHODS

Detailed methods are provided in the online version of this paper and include the following:

- KEY RESOURCES TABLE
- EXPERIMENTAL MODEL AND STUDY PARTICIPANT DETAILS
  - Cell lines
- METHOD DETAILS
  - Plasmid construction
  - Luciferase assay
  - RNA interference
  - Antibodies
  - Immunoblotting
  - Analyzing the oxidation status of FLuc* in cells
- QUANTIFICATION AND STATISTICAL ANALYSIS

SUPPLEMENTAL INFORMATION

Supplemental information can be found online at https://doi.org/10.1016/j.isci.2024.111189.

Received: April 8, 2024
Revised: September 1, 2024
Accepted: October 14, 2024
Published: October 16, 2024

REFERENCES

1. Chitwood, P.J., and Hegde, R.S. (2019). The Role of EMC during Membrane Protein Biogenesis. Trends Cell Biol. *29*, 371–384. https://doi.org/10.1016/j.tcb.2019.01.007.
2. Rapoport, T.A., Li, L., and Park, E. (2017). Structural and mechanistic insights into protein translocation. Annu. Rev. Cell Dev. Biol. *33*, 369–390. https://doi.org/10.1146/annurev-cellbio-100616-060439.
3. Feige, M.J., Braakman, I., and Hendershot, L.M. (2018). Disulfide Bonds in Protein Folding and Stability. In Oxidative Folding of Proteins: Basic Principles, Cellular Regulation and Engineering, M.J. Feige, ed. (Royal Society of Chemistry), pp. 1–33. https://doi.org/10.1039/9781782629900-00001.
4. Lang, S., Pfeffer, S., Lee, P.H., Cavalié, A., Helms, V., Förster, F., and Zimmermann, R. (2017). An update on Sec 61 channel functions, mechanisms, and related diseases. Front. Physiol. *8*, 887. https://doi.org/10.3389/fphys.2017.00887.
5. Anelli, T., and Sitia, R. (2018). Mechanisms of Oxidative Protein Folding and Thiol-dependent Quality Control: Tales of Cysteines and Cystines. In Oxidative Folding of Proteins: Basic Principles, Cellular Regulation and Engineering, M.J. Feige, ed. (Royal Society of Chemistry), pp. 249–266. https://doi.org/10.1039/9781788013253-00249.
6. Ellgaard, L., McCaul, N., Chatsisvili, A., and Braakman, I. (2016). Co- and Post-Translational Protein Folding in the ER. Traffic *17*, 615–638. https://doi.org/10.1111/tra.12392.
7. Fass, D., and Thorpe, C. (2018). Chemistry and Enzymology of Disulfide Cross-Linking in Proteins. Chem. Rev. *118*, 1169–1198. https://doi.org/10.1021/acs.chemrev.7b00123.
8. Okumura, M., Kadokura, H., and Inaba, K. (2015). Structures and functions of protein disulfide isomerase family members involved in proteostasis in the endoplasmic reticulum. Free Radic. Biol. Med. *83*, 314–322. https://doi.org/10.1016/j.freeradbiomed.2015.02.010.
9. Beckwith, J. (2013). Fifty years fused to lac. Annu. Rev. Microbiol. *67*, 1–19. https://doi.org/10.1146/annurev-micro-092412-155732.
10. Bardwell, J.C., McGovern, K., and Beckwith, J. (1991). Identification of a protein required for disulfide bond formation in vivo. Cell *67*, 581–589. https://doi.org/10.1016/0092-8674(91)90532-4.
11. Grauschopf, U., Winther, J.R., Korber, P., Zander, T., Dallinger, P., and Bardwell, J.C. (1995). Why is DsbA such an oxidizing disulfide catalyst? Cell *83*, 947–955. https://doi.org/10.1016/0092-8674(95)90210-4.
12. Kadokura, H., Tian, H., Zander, T., Bardwell, J.C.A., and Beckwith, J. (2004). Snapshots of DsbA in Action: Detection of Proteins in the Process of Oxidative Folding. Science *303*, 534–537. https://doi.org/10.1126/science.1091724.
13. Silhavy, T.J., and Mitchell, A.M. (2019). Genetic Analysis of Protein Translocation. Protein J. *38*, 217–228. https://doi.org/10.1007/s10930-019-09813-y.
14. Tian, H., Boyd, D., and Beckwith, J. (2000). A mutant hunt for defects in membrane protein assembly yields mutations affecting the bacterial signal recognition particle and Sec machinery. Proc. Natl. Acad. Sci. USA *97*, 4730–4735. https://doi.org/10.1073/pnas.090087297.
15. Landeta, C., Blazyk, J.L., Hatahet, F., Meehan, B.M., Eser, M., Myrick, A., Bronstain, L., Minami, S., Arnold, H., Ke, N., et al. (2015). Compounds targeting disulfide bond forming enzyme DsbB of Gram-negative bacteria. Nat. Chem. Biol. *11*, 292–298. https://doi.org/10.1038/nchembio.1752.
16. Kadokura, H., and Beckwith, J. (2010). Mechanisms of oxidative protein folding in the bacterial cell envelope. Antioxidants Redox Signal. *13*, 1231–1246. https://doi.org/10.1089/ars.2010.3187.
17. Lemke, E.A., and Schultz, C. (2011). Principles for designing fluorescent sensors and reporters. Nat. Chem. Biol. *7*, 480–483. https://doi.org/10.1038/nchembio.620.

18. Lukyanov, K.A., and Belousov, V.V. (2014). Genetically encoded fluorescent redox sensors. Biochim. Biophys. Acta *1840*, 745–756. https://doi.org/10.1016/j.bbagen.2013.05.030.
19. Hanson, G.T., Aggeler, R., Oglesbee, D., Cannon, M., Capaldi, R.A., Tsien, R.Y., and Remington, S.J. (2004). Investigating Mitochondrial Redox Potential with Redox-sensitive Green Fluorescent Protein Indicators. J. Biol. Chem. *279*, 13044–13053. https://doi.org/10.1074/jbc.M312846200.
20. Meyer, A.J., and Dick, T.P. (2010). Fluorescent Protein-Based Redox Probes. Antioxidants Redox Signal. *13*, 621–650.
21. Lohman, J.R., and Remington, S.J. (2008). Development of a family of redox-sensitive green fluorescent protein indicators for use in relatively oxidizing subcellular environments. Biochemistry *47*, 8678–8688. https://doi.org/10.1021/bi800498g.
22. van Lith, M., Tiwari, S., Pediani, J., Milligan, G., and Bulleid, N.J. (2011). Real-time monitoring of redox changes in the mammalian endoplasmic reticulum. J. Cell Sci. *124*, 2349–2356. https://doi.org/10.1242/jcs.085530.
23. Avezov, E., Cross, B.C.S., Kaminski Schierle, G.S., Winters, M., Harding, H.P., Melo, E.P., Kaminski, C.F., and Ron, D. (2013). Lifetime imaging of a fluorescent protein sensor reveals surprising stability of ER thiol redox. J. Cell Biol. *201*, 337–349. https://doi.org/10.1083/jcb.201211155.
24. Hoseki, J., Oishi, A., Fujimura, T., and Sakai, Y. (2016). Development of a stable ERroGFP variant suitable for monitoring redox dynamics in the ER. Biosci. Rep. *36*, e00316. https://doi.org/10.1042/BSR20160027.
25. Roberts, B.S., Babilonia-Rosa, M.A., Broadwell, L.J., Wu, M.J., and Neher, S.B. (2018). Lipase maturation factor 1 affects redox homeostasis in the endoplasmic reticulum. EMBO J. *37*, e97379. https://doi.org/10.15252/embj.201797379.
26. Zhang, J., Zhu, Q., Wang, X., Yu, J., Chen, X., Wang, J., Wang, X., Xiao, J., Wang, C.C., and Wang, L. (2018). Secretory kinase Fam20C tunes endoplasmic reticulum redox state via phosphorylation of Ero1α. EMBO J. *37*, e98699. https://doi.org/10.15252/embj.201798699.
27. Gupta, R., Kasturi, P., Bracher, A., Loew, C., Zheng, M., Villella, A., Garza, D., Hartl, F.U., and Raychaudhuri, S. (2011). Firefly luciferase mutants as sensors of proteome stress. Nat. Methods *8*, 879–884. https://doi.org/10.1038/nmeth.1697.
28. Singh, A., Manjunath, L.E., Kundu, P., Sahoo, S., Das, A., Suma, H.R., Fox, P.L., and Eswarappa, S.M. (2019). Let-7a-regulated translational readthrough of mammalian AGO1 generates a micro RNA pathway inhibitor. EMBO J. *38*, e100727. https://doi.org/10.15252/embj.2018100727.
29. Yasunaga, M., Murotomi, K., Abe, H., Yamazaki, T., Nishii, S., Ohbayashi, T., Oshimura, M., Noguchi, T., Niwa, K., Ohmiya, Y., and Nakajima, Y. (2015). Highly sensitive luciferase reporter assay using a potent destabilization sequence of calpain 3. J. Biotechnol. *194*, 115–123. https://doi.org/10.1016/j.jbiotec.2014.12.004.
30. Vermeire, K., Bell, T.W., Van Puyenbroeck, V., Giraut, A., Noppen, S., Liekens, S., Schols, D., Hartmann, E., Kalies, K.U., and Marsh, M. (2014). Signal Peptide-Binding Drug as a Selective Inhibitor of Co-Translational Protein Translocation. PLoS Biol. *12*, e1002011. https://doi.org/10.1371/journal.pbio.1002011.
31. McNabb, D.S., Reed, R., and Marciniak, R.A. (2005). Dual luciferase assay system for rapid assessment of gene expression in Saccharomyces cerevisiae. Eukaryot. Cell *4*, 1539–1549. https://doi.org/10.1128/EC.4.9.1539-1549.2005.
32. Neefjes, M., Housmans, B.A.C., van den Akker, G.G.H., van Rhijn, L.W., Welting, T.J.M., and van der Kraan, P.M. (2021). Reporter gene comparison demonstrates interference of complex body fluids with secreted luciferase activity. Sci. Rep. *11*, 1359. https://doi.org/10.1038/s41598-020-80451-6.
33. Su, Y., Walker, J.R., Park, Y., Smith, T.P., Liu, L.X., Hall, M.P., Labanieh, L., Hurst, R., Wang, D.C., Encell, L.P., et al. (2020). Novel NanoLuc substrates enable bright two-population bioluminescence imaging in animals. Nat. Methods *17*, 852–860. https://doi.org/10.1038/s41592-020-0889-6.
34. Oba, Y., Iida, K., and Inouye, S. (2009). Functional conversion of fatty acyl-CoA synthetase to firefly luciferase by site-directed mutagenesis: A key substitution responsible for luminescence activity. FEBS Lett. *583*, 2004–2008. https://doi.org/10.1016/j.febslet.2009.05.018.
35. Nakamura, D., Tsuru, A., Ikegami, K., Imagawa, Y., Fujimoto, N., and Kohno, K. (2011). Mammalian ER stress sensor IRE1β specifically down-regulates the synthesis of secretory pathway proteins. FEBS Lett. *585*, 133–138. https://doi.org/10.1016/j.febslet.2010.12.002.
36. Loening, A.M., Fenn, T.D., Wu, A.M., and Gambhir, S.S. (2006). Consensus guided mutagenesis of Renilla luciferase yields enhanced stability and light output. Protein Eng. Des. Sel. *19*, 391–400. https://doi.org/10.1093/protein/gzl023.
37. Kaup, M., Saul, V.V., Lusch, A., Dörsing, J., Blanchard, V., Tauber, R., and Berger, M. (2011). Construction and analysis of a novel peptide tag containing an unnatural N-glycosylation site. FEBS Lett. *585*, 2372–2376. https://doi.org/10.1016/j.febslet.2011.06.010.
38. Musik, J.E., Zalucki, Y.M., Beacham, I.R., and Jennings, M.P. (2022). The role of signal sequence proximal residues in the mature region of bacterial secreted proteins in E. coli. Biochim. Biophys. Acta Biomembr. *1864*, 184000. https://doi.org/10.1016/j.bbamem.2022.184000.
39. Sun, S., Li, X., and Mariappan, M. (2023). Signal sequences encode information for protein folding in the endoplasmic reticulum. J. Cell Biol. *222*, e202203070. https://doi.org/10.1083/jcb.202203070.
40. Pauwels, E., Schülein, R., and Vermeire, K. (2021). Inhibitors of the Sec61 complex and novel high throughput screening strategies to target the protein translocation pathway. Int. J. Mol. Sci. *22*, 12007. https://doi.org/10.3390/ijms222112007.
41. Bulleid, N.J., and Ellgaard, L. (2011). Multiple ways to make disulfides. Trends Biochem. Sci. *36*, 485–492. https://doi.org/10.1016/j.tibs.2011.05.004.
42. Kanemura, S., Sofia, E.F., Hirai, N., Okumura, M., Kadokura, H., and Inaba, K. (2020). Characterization of the endoplasmic reticulum–resident peroxidases GPx7 and GPx8 shows the higher oxidative activity of GPx7 and its linkage to oxidative protein folding. J. Biol. Chem. *295*, 12772–12785. https://doi.org/10.1074/jbc.ra120.013607.
43. Okumura, M., Kadokura, H., Hashimoto, S., Yutani, K., Kanemura, S., Hikima, T., Hidaka, Y., Ito, L., Shiba, K., Masui, S., et al. (2014). Inhibition of the functional interplay between endoplasmic reticulum (ER) Oxidoreduclin-1α (Ero1α) and protein-disulfide isomerase (PDI) by the endocrine disruptor bisphenol A. J. Biol. Chem. *289*, 27004–27018. https://doi.org/10.1074/jbc.M114.564104.
44. Appenzeller-Herzog, C., Riemer, J., Christensen, B., Sørensen, E.S., and Ellgaard, L. (2008). A novel disulphide switch mechanism in Ero1α balances ER oxidation in human cells. EMBO J. *27*, 2977–2987. https://doi.org/10.1038/emboj.2008.202.
45. Araki, K., and Inaba, K. (2012). Structure, mechanism, and evolution of ero1 family enzymes. Antioxidants Redox Signal. *16*, 790–799. https://doi.org/10.1089/ars.2011.4418.
46. Baker, K.M., Chakravarthi, S., Langton, K.P., Sheppard, A.M., Lu, H., and Bulleid, N.J. (2008). Low reduction potential of Ero1α regulatory disulphides ensures tight control of substrate oxidation. EMBO J. *27*, 2988–2997. https://doi.org/10.1038/emboj.2008.230.
47. Kadokura, H., Dazai, Y., Fukuda, Y., Hirai, N., Nakamura, O., and Inaba, K. (2020). Observing the nonvectorial yet cotranslational folding of a multidomain protein, LDL receptor, in the ER of mammalian cells. Proc. Natl. Acad. Sci. USA *117*, 16401–16408. https://doi.org/10.1073/pnas.2004606117.
48. Cao, X., Lilla, S., Cao, Z., Pringle, M.A., Oka, O.B.V., Robinson, P.J., Szmaja, T., Van Lith, M., Zanivan, S., and Bulleid, N.J. (2020). The mammalian cytosolic thioredoxin reductase pathway acts via a membrane protein to reduce ER-localised proteins. J. Cell Sci. *133*, jcs241976. https://doi.org/10.1242/jcs.241976.
49. Poet, G.J., Oka, O.B., van Lith, M., Cao, Z., Robinson, P.J., Pringle, M.A., Arnér, E.S., and Bulleid, N.J. (2017). Cytosolic thioredoxin reductase 1 is required for correct disulfide formation in the ER. EMBO J. *36*, 693–702. https://doi.org/10.15252/evmbj.201695336.
50. Mittal, A., Manjunath, K., Ranjan, R.K., Kaushik, S., Kumar, S., and Verma, V. (2020). COVID-19 pandemic: Insights into structure, function, and hACE2 receptor recognition by SARS-CoV-2. PLoS Pathog. *16*, e1008762.
51. Kishimoto, T., and Kang, S. (2022). IL-6 Revisited: From Rheumatoid Arthritis to CAR T Cell Therapy and COVID-19. Annu. Rev. Immunol. *40*, 323–348. https://doi.org/10.1371/journal.ppat.1008762.
52. Ota, T., Suzuki, Y., Nishikawa, T., Otsuki, T., Sugiyama, T., Irie, R., Wakamatsu, A., Hayashi, K., Sato, H., Nagai, K., et al. (2004). Complete sequencing and characterization of 21,243 full-length human cDNAs. Nat. Genet. *36*, 40–45. https://doi.org/10.1038/ng1285.

STAR★METHODS

KEY RESOURCES TABLE

REAGENT or RESOURCE	SOURCE	IDENTIFIER
Antibodies		
Mouse monoclonal anti-FLAG (clone M2), horseradish peroxidase-conjugated	Sigma-Aldrich	Cat#A8592; RRID: AB_439702
Mouse monoclonal anti-GAPDH (clone GAPDH-71.1), horseradish peroxidase-conjugated	Sigma-Aldrich	Cat#G9295; RRID: AB_1078992
Mouse monoclonal anti-SRP54 (clone 30/SRP54)	BD Biosciences	Cat#610940; RRID: AB_398254
Rabbit polyclonal anti-LMF1	This paper	N/A
Rat monoclonal anti-PA tag (clone NZ-1), horseradish peroxidase-conjugated	Fujifilm Wako	Cat#015-25951
m-IgG Fc BP, horseradish peroxidase-conjugated	Santa Cruz Biotechnology	Cat#sc-525409; RRID: AB_3101828
Mouse anti-Rabbit IgG, horseradish peroxidase-conjugated	Santa Cruz Biotechnology	Cat#sc-2357; RRID: AB_628497
Bacterial and virus strains		
E-cos™ Escherichia coli BL21 (DE3)	Nippon Gene	Cat#318-06531
Chemicals, peptides, and recombinant proteins		
Benzamide	Nacalai Tesque	Cat#04011-82
Bisphenol A	Nacalai Tesque	Cat#05032-24
CNBr-activated Sepharose 4B	Sigma Aldrich	Cat#17-0430-01
Cyclotriazadisulfonamide (CADA)	Sigma Aldrich	Cat#534337
Dithiothreitol (DTT)	Nacalai Tesque	Cat#14128-91
Diamide	Sigma Aldrich	Cat#D3648
DMEM	Nacalai Tesque	Cat#08458
Endoglycosidase H (Endo H)	New England Biolabs	Cat#P0702S
Effectene	Qiagen	Cat#301425
Fetal bovine serum (FBS)	Nichirei Biosciences	Cat#175012
Gibson Assembly Master Mix	New England Biolabs	Cat#E2611
Lipofectamine RNAiMAX	Thermo Fisher Scientific	Cat#13778150
Ni-NTA agarose	Qiagen	Cat#30210
nProtein A Sepharose™ 4 FAST FLOW	GE Healthcare	Cat#17-5280-01
Nonidiet P40 (NP-40)	Nacalai Tesque	Cat#23640-65
Opti-MEM	Gibco	Cat#31985-070
Pepstatin A	Nacalai Tesque	Cat#26435-52
Phenylmethylsulfonyl fluoride (PMSF)	Nacalai Tesque	Cat#27327-81
Peptide -*N*-Glycosidase F (PNGase F)	New England Biolabs	Cat#: P0704S
QuikChange Lightning Site-Directed Mutagenesis Kit	Agilent	Cat#210518,
QuikChange Lightning Multi Site-Directed Mutagenesis Kit	Agilent	Cat#210515
Sunbright® ME-020MA (Mal-PEG 2000)	NOF	Cat#ME-020MA
Critical commercial assays		
Chemi-Lumi One Ultra	Nacalai Tesque	Cat#11644-24
Clarity Western ECL substrate	Bio-Rad	Cat#1705061

(*Continued on next page*)

Continued

REAGENT or RESOURCE	SOURCE	IDENTIFIER
Dual-Luciferase® Reporter 1000 Assay System	Promega	Cat#E1980
EZ-PCR Mycoplasma Detection Kit	Biological Industries	Cat#20-700-20
Experimental models: Cell lines		
HeLa Tet-Off (HeLa cells)	Clontech	Cat#C3005-1; RRID: CVCL_V352
Oligonucleotides		
Control siRNA	Thermo Fisher Scientific (Ambion®)	Cat#4390843
SRP54 siRNA #2 (siSRP54 #2) : 5′-GAAGGAGUAGAGAAAUUUATT-3′; 5′-UAAAUUUCUCUACUCCUUCAG-3′	Thermo Fisher Scientific (Ambion®)	Cat#s57088
SRP54 siRNA #3 (siSRP54 #3): 5′- GACUGAUAGAUAAAGUCAATT-3′ 5′-UUGACUUUAUCUAUCAGUCCT-3	Thermo Fisher Scientific (Ambion®)	Cat#s57090
LMF1 siRNA (siLMF1): 5′-GGCAGGUCAUGAACACCCATT-3′ 5′-UGGGUGUUCAUGACCUGCCTG-3′	Thermo Fisher Scientific (Ambion®)	Cat#s34950
See Tables S3–S5 for primers used for plasmid construction	This study	N/A
Recombinant DNA		
pcDNA3.1^{+}	Invitrogen	Cat#V79020
pET15b	Novagen	Cat#69661
pRL-SV40	Promega	Cat#E2231
pFL-SV40-ER [pRL-SV40 ΔRLuc Calr (17 aa)-FLuc-KDEL w/o N197Q]	Nakamura et al.[35]	N/A
pHK960 [pRL-SV40 ΔRLuc Calr (17 aa)-FLuc-KDEL]	This paper	N/A
pHK961 [pRL-SV40 ΔRLuc FLuc-KDEL WT]	This paper	N/A
pHK1023 [pRL-SV40 ΔRLuc FLuc-KDEL S85C]	This paper	N/A
pHK1024 [pRL-SV40 ΔRLuc FLuc-KDEL L93C]	This paper	N/A
pHK1025 [pRL-SV40 ΔRLuc FLuc-KDEL I145C]	This paper	N/A
pHK1026 [pRL-SV40 ΔRLuc FLuc-KDEL A222C]	This paper	N/A
pHK1027 [pRL-SV40 ΔRLuc FLuc-KDEL V362C]	This paper	N/A
pHK1032 [pRL-SV40 ΔRLuc FLuc-KDEL V61C]	This paper	N/A
pHK1033 [pRL-SV40 ΔRLuc FLuc-KDEL V128C]	This paper	N/A
pHK1034 [pRL-SV40 ΔRLuc FLuc-KDEL S163C]	This paper	N/A
pHK1035 [pRL-SV40 ΔRLuc FLuc-KDEL I282C]	This paper	N/A
pHK1036 [pRL-SV40 ΔRLuc FLuc-KDEL S314C]	This paper	N/A
pHK1037 [pRL-SV40 ΔRLuc FLuc-KDEL N463C]	This paper	N/A
pHK1042 [pRL-SV40 ΔRLuc FLuc-KDEL L115C]	This paper	N/A
pHK1110 [pRL-SV40 ΔRLuc Calr (17 aa)-FLuc-KDEL +8 Cys]	This paper	N/A
pHK1548 [pRL-SV40 ΔRLuc Calr (17 aa)-FLuc*]	This paper	N/A
pSY107 [pRL-SV40 ΔRLuc Calr (40 aa)-FLuc*]	This paper	N/A
pSY108 [pRL-SV40 ΔRLuc CD4 (40 aa)-FLuc*]	This paper	N/A
pSY109 [pRL-SV40 ΔRLuc bPRL (40 aa)-FLuc*]	This paper	N/A
pHK1411 [pRL-SV40 ΔRLuc Calr (40 aa)-FLuc* (−2 Cys)]	This paper	N/A
pHK1608 [pRL-SV40 ΔRLuc Met-FLuc*]	This paper	N/A
pHK1061 [pcDNA3.1 Ero1α-Myc]		N/A
pHK1124 [pcDNA3.1 Ero1α-Myc C104A C131A (hyperactive Ero1α)]	This paper	N/A

(*Continued on next page*)

Continued

REAGENT or RESOURCE	SOURCE	IDENTIFIER
pHK1407 [pcDNA3.1$^+$ siRNA-resistant mSRP54]	This paper	N/A
pHK1434 [pcDNA3.1$^+$ LMF1]	This paper	N/A
pHK1514 [pcDNA3.1$^+$ siRNA-resistant PA-LMF1]	This paper	N/A
pHK1616 [pcDNA3.1$^+$ with siRNA-resistant LMF1]	This paper	N/A
pHK1486 [pET15b C-terminal 179 amino acid residues of LMF1 containing a hexahistidiine tag at its C-terminus]	This paper	N/A
See Table S2 for detailed information on plasmids constructed in this study	This paper	N/A
Software and algorithms		
GraphPad Prism 10.2	GraphPad Software	RRID: SCR_002798

EXPERIMENTAL MODEL AND STUDY PARTICIPANT DETAILS

Cell lines

HeLa cells (HeLa Tet-off; Clontech) were maintained in Dulbecco's modified Eagle's medium (DMEM) (Nacalai Tesque) supplemented with 10% fetal bovine serum (FBS) Nichirei Biosciences) at 37°C in 5% CO_2 air. The cell line has not been authenticated in this study. The absence of mycoplasma in cells was confirmed using EZ-PCR Mycoplasma Detection Kit (Biological Industries).

METHOD DETAILS

Plasmid construction

Detailed information on the plasmids constructed in this study are listed in Table S2. Plasmids listed in Table S3 were constructed by site-directed mutagenesis using the indicated template, primer(s) and either the QuikChange Lightning Site-Directed Mutagenesis Kit (Agilent) or the QuikChange Lightning Multi Site-Directed Mutagenesis Kit (Agilent). Plasmids listed in Table S4 were constructed by assembling two fragments using the Gibson Assembly Master Mix (New England Biolabs). These fragments were amplified from templates using primer sets indicated in the table. The sequences of oligonucleotides (primers) used for plasmid construction are listed in Table S5. The other plasmids were created as follow. pFL-SV40-ER is a derivative of pRL-SV40 (Promega) designed to express an ER-localized FLuc under the control of the SV40 promoter. This protein was constructed by fusing the human calreticulin signal sequence (17 amino acids) and the KDEL motif at the N- and C-termini of FLuc from *P. pyralis*, respectively[35] and was named as Calr (17 aa)-FLuc-KDEL w/o N197Q. To remove the signal sequence from the FLuc construct in pFL-SV40-ER, the latter plasmid was used as a template for PCR amplification using FLucH21 and FLucH22, digested at NheI in the primers, and self-ligated to yield pHK955. To insert a 22-amino acid sequence containing an N-glycosylation site[37] between the FLuc and KDEL sequences in pHK1110, pHK1110 was used as the template for PCR amplification with FLucH76 and FLucH78, and with FLucH77, and FLucH79. The products were digested at NgoMIV, and BglII sites in the primers and ligated to yield pHK1126. To introduce an additional N-glycosylation site after the FLuc sequence of pHK1126, two oligonucleotides, FLucH92 and FLucH93, were annealed and inserted into the XhoI site of pHK1126, yielding pHK1138. A human cDNA clone for Ero1α (IRAK013H07) and a human cDNA fragment encoding the C-terminal 490 amino acid residues of LMF1 (IRAK014N12) were obtained from the RIKEN BioResource Research Center.[52] To construct pHK1061, which expresses hEro1α-Myc, a DNA fragment encoding hEro1α-Myc was amplified from IRAK013H07 using primers hEro1LaH1, and hEro1LaH2, digested with KpnI, and XbaI in primers, and cloned into pcDNA3.1$^+$ (Invitrogen). Plasmid pHK1434 is a derivative of pcDNA3.1$^+$ that expresses human LMF1. It was constructed by assembling three DNA fragment fragments: a 5.4-kb fragment amplified from pcDNA3.1$^+$ using primers (pcDNAH1, and pcDNAH2), a 2.1-kb fragment amplified from IRAK014N12 (see above) using primers (hLMF1H3, and hLMF1H4), and a 267-bp fragment amplified from synthetic DNA (encoding the N-terminal 77 amino acid residues of human LMF1) using primers (hLMF1H1 and hLMF1H2). Plasmid pcDNA3.1$^+$-mSRP54, encoding mouse SRP54, was kindly provided by Satoshi Kanda, a former lab member of Kenji Kohno Lab. Plasmid pNH101 is a derivative of pcDNA3.1$^+$ that expresses siRNA-resistant SRP54. It was constructed by assembling these fragments: a 4.0-kb, a 405-bp, and a 2.6-kb fragment amplified from pcDNA3.1$^+$-mSRP54 using the following primer sets: (mSRP54H1, and NeoRH1), (mSRP54H2 and mSPR54H3), and (mSRP54H4 and NeoRH2), respectively. All clones were verified by sequencing the entire ORF.

Luciferase assay

HeLa cells, cultured as described above, were seeded at a density of 1.5 × 10^5 cells/well in a 6-well plate. After 24 h, cells were transfected, unless otherwise specified, with 95 ng of an appropriate FLuc-based reporter plasmid and 5 ng of pRL-SV40 (Promega) expressing *Renilla* luciferase (RLuc) using Effectene (Qiagen) according to the manufacturer's instructions, with the exception that Opti-MEM (Gibco) was used to dilute DNA. Effectene was used at a concentration of 12.5 μL/μg DNA. Twenty-four hours post-transfection, cells were washed twice with phosphate-buffered saline (PBS) [137 mM NaCl, 2.7 mM KCl, 8 mM Na_2HPO_4, 1.5 mM KH_2PO_4 (pH7.4)] and lysed with 500 μL of cell lysis

buffer [PBS, 1% Nonidiet P40 (NP40) (Nacalai Tesque), 1 mM phenylmethylsulfonyl fluoride (PMSF) (Nacalai Tesque), 1 mM benzamide (Nacalai Tesque) and 1 μg/mL pepstatin A (Nacalai Tesque)]. A 2 μL aliquot of the lysate was subjected to a dual luciferase assay using a luminometer (ATTO model AB-2270) to measure FLuc and RLuc activities. For this purpose, the Dual Luciferase Reporter System (Promega) was used. Briefly, 50 μL of firefly luciferase reagent (LAR II) was added to the sample and mixed immediately to measure luminescence (FLuc activity) for 10 s. Subsequently, 50 μL of *Renilla* luciferase reagent and firefly quenching reagent (Stop & Glo) was added to the sample to measure luminescence (RLuc activity) for 10 s. Relative FLuc activity was calculated by dividing FLuc activity by RLuc activity (FLuc/RLuc). For data comparison, values were further normalized to those of mock-treated samples and expressed as normalized relative FLuc activity.

RNA interference

The Silencer Select siRNAs targeting human SRP54 and LMF1 were obtained from Thermo Fisher Scientific, and delivered into cells using Lipofectamine RNAiMAX (Thermo Fisher Scientific) following the manufacturer's reverse transfection protocol. The siRNA was used at a final concentration of 20 nM, and cells were seeded at a density of 1.5×10^5 cells/well in a 6-well plate. Twenty-four hours after siRNA transfection, reporter plasmids were introduced into the cells for the luciferase assay, as described above.

Antibodies

Mouse anti-SRP54 antibody (BD Biosciences), horseradish peroxidase-conjugated anti-GAPDH antibody (Sigma-Aldrich) and anti-FLAG M2 antibody (Sigma-Aldrich), and rabbit anti-LMF1 antibody were used for immunoblotting. Rabbit anti-LMF1 antibody was generated as follows: The C-terminal 179 amino acid residues of human LMF1, including a hexahistidine tag at its C-terminus, were expressed from pHK1485, a derivative of pET15b (Novagen), in BL21 (DE3) (Nippon Gene). Cells were suspended in lysis buffer [50 mM Tris-HCl (pH8.1), 300 mM NaCl, and 0.5 mM EDTA], lysed using a French Pressure Cell, and centrifuged at 10,000 x *g* at 4°C for 20 min to obtain the C-terminal domain of LMF1 in the pellet. The protein was then solubilized in solubilization buffer [50 mM Tris-HCl (pH8.1), 300 mM NaCl, and 6 M guanidine HCl] and subjected to affinity purification using Ni-NTA agarose (Qiagen) following the manufacturer's protocol. Rabbit immunization with the purified protein was performed by Eurofins. Anti-LMF1 antibody in the antiserum was purified first with the antigen conjugated to CNBr-activated Sepharose 4B (Sigma-Aldrich) and then with nProtein A Sepharose 4 FAST FLOW (GE Healthcare). The resulting affinity-purified immunoglobulin G was used as an antibody to detect endogenous LMF1 in HeLa cells.

Immunoblotting

Proteins were separated using 10% sodium dodecyl sulfate (SDS)-polyacrylamide gel electrophoresis (SDS-PAGE), transferred to an Immobilon-P membrane (Millipore), incubated with a primary antibody and then with an appropriate secondary antibody if the primary antibody was not conjugated with horseradish peroxidase, and detected using Clarity Western ECL Substrate (Bio-Rad), or Chemi-Lumi One Ultra (Nacali Tesque) and ChemiDoc Touch Imaging System (Bio-Rad) or LAS 4000 MC (Fujifilm). Second antibodies used were horseradish peroxidase-conjugated mouse anti-Rabbit IgG (Santa Cruz Biotechnology), and horseradish peroxidase-conjugated *m*-IgG Fc BP (Santa Cruz Biotechnology) for detection with anti-LMF1 and anti-SRP54 antibodies (see above), respectively.

Analyzing the oxidation status of FLuc* in cells

To analyze the redox states of FLuc* in cells, the free cysteine residues of cellular proteins were acid-trapped and alkylated with the high molecular mass reagent Mal-PEG 2000 (SUNBRIGHT ME-020MA) (NOF).[43] Briefly, cells expressing an appropriate reporter were washed twice with PBS and treated directly with ice-cold 10% trichloroacetic acid (TCA). After a 20-min incubation on ice, cells were collected, washed twice with ice-cold acetone to remove acid, and dissolved in alkylation buffer [100 mM Tris-HCl (pH 7.2), 2% SDS] containing 5.5 mM Mal-PEG 2000 and protease inhibitors (10 μg/mL pepstatin A, 1 mM benzamide, and 1 mM phenylmethylsulfonyl fluoride). The samples were then agitated for 20 min and incubated for an additional 30 min at 37°C to obtain Mal-PEG 2000-treated cell lysates. Proteins from the resulting cell lysates were separated using 10% SDS-PAGE under reducing conditions and subjected to immunoblotting using horseradish peroxidase-conjugated anti-FLAG M2 antibody as described above.

QUANTIFICATION AND STATISTICAL ANALYSIS

Statistical analyses were conducted with Prism software version 7.0a, 9.20, 9.3. or 10.0.2 (GraphPad Software), using a two-tailed unpaired t-test or one-way ANOVA followed by Dunnett's test or Tukey's test for comparison of multiple datasets. Data represent the means of the indicated number of independent experiments. Error bars indicate the standard deviation (SD). A *p*-value less than 0.05 was considered significant.